η and η' Mesons from Lattice QCD

N. H. Christ,[1] C. Dawson,[2] T. Izubuchi,[3,4] C. Jung,[3] Q. Liu,[1] R. D. Mawhinney,[1] C. T. Sachrajda,[5] A. Soni,[3] and R. Zhou[6]

(RBC and UKQCD Collaborations)

[1]*Physics Department, Columbia University, New York, New York 10027, USA*
[2]*Department of Physics, University of Virginia, 382 McCormick Road, Charlottesville, Virginia 22904-4714, USA*
[3]*Brookhaven National Laboratory, Upton, New York 11973, USA*
[4]*RIKEN-BNL Research Center, Brookhaven National Laboratory, Upton, New York 11973, USA*
[5]*School of Physics and Astronomy, University of Southampton, Southampton SO17 1BJ, United Kingdom*
[6]*Physics Department, University of Connecticut, Storrs, Connecticut 06269-3046, USA*
(Received 24 February 2010; published 8 December 2010)

The large mass of the ninth pseudoscalar meson, the η', is believed to arise from the combined effects of the axial anomaly and the gauge field topology present in QCD. We report a realistic, 2 + 1-flavor, lattice QCD calculation of the η and η' masses and mixing which confirms this picture. The physical eigenstates show small octet-singlet mixing with a mixing angle of $\theta = -14.1(2.8)°$. Extrapolation to the physical light quark mass gives, with statistical errors only, $m_\eta = 573(6)$ MeV and $m_{\eta'} = 947(142)$ MeV, consistent with the experimental values of 548 and 958 MeV.

DOI: 10.1103/PhysRevLett.105.241601 PACS numbers: 12.38.Gc, 11.15.Ha, 11.30.Rd, 14.40.Be

The relatively large mass of the ninth pseudoscalar meson, the η', provides a significant challenge for quantum chromodynamics (QCD), the component of the standard model which describes the interactions of quarks and gluons. On a naive classical level, there are nine conserved axial-vector currents. Given the vacuum breaking of the symmetries which these currents generate, this should imply the existence of nine Goldstone bosons, a conclusion inconsistent with the large splitting between the 8 octet mesons $\pi^\pm$, π^0, $K^\pm$, K^0, $\bar{K}^0$, and η and the singlet η' [1]. Unique among these nine currents, the U(1) axial-vector current, corresponding to the singlet η' meson, has an anomalous divergence at the quantum level. However, to arbitrary order in perturbation theory this anomalous divergence vanishes at zero momentum, continuing to imply that the masses of all nine pseudoscalar mesons should vanish in the limit of a vanishing quark mass. It is only with the discovery of instanton configurations with nontrivial topology [2] that a mechanism [3] became available that could explain the large η' mass.

While these important developments suggest a possible consistency between QCD and the value of the η' mass, a direct demonstration of the required anomaly-driven, octet-singlet splitting has been lacking. In this Letter, we present the first such demonstration in the realistic case of three light dynamical quarks.

The critical role of disconnected diagrams in the study of the η and η' and the severe difficulties they introduce have been recognized for more than 15 years [4,5]. Positivity requires the quark propagators that appear in the connected diagrams to decrease exponentially with increasing time separation. For mesons this falloff roughly matches the exponential time dependence of the massive, Euclidean-space meson propagator, and good numerical signals can be seen over a large range of times. For terms in which the source and sink of the meson propagator are not joined by quark propagators, the needed exponential decrease comes from increasingly large statistical cancellations implying a rapidly vanishing signal-to-noise ratio. These difficulties have impeded earlier work [6–9] on this topic which has employed indirect methods or not examined the physical case of up, down, and strange dynamical quarks; see also Ref. [10].

Simulation details.—Our calculation uses the Iwasaki gauge and domain wall fermion actions, a $16^3 \times 32$ space-time volume with a fifth-dimensional extent of 16 and $\beta = 2.13$, giving an inverse lattice spacing $1/a = 1.73(3)$ GeV [11]. We analyze three ensembles of gauge configurations with light sea quark mass $m_l = 0.01$, 0.02, and 0.03 [12]. (All dimensionful quantities are given in lattice units except when physical units are declared.) These values of m_l yield pion masses of 421, 561, and 672 MeV, respectively. The 0.01 and 0.02 ensembles were generated by using the physical strange quark mass $m_s = 0.032$ [13]. The $m_l = 0.03$ ensemble was reported as RHMC II in Ref. [11] with $m_s = 0.04$. For this ensemble we use reweighting to change m_s from 0.04 to 0.032 in 20 mass steps [14].

We use a Coulomb gauge fixed wall source and sink for the quark propagators. Because of the difficulty of computing

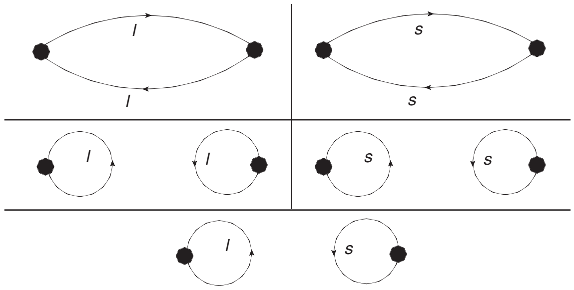

FIG. 1. Five diagrams appearing in the η and η' correlation functions. They are $\mathcal{C}_{ll}(t)$, $\mathcal{C}_{ss}(t)$, $\mathcal{D}_{ll}(t)$, $\mathcal{D}_{ss}(t)$, and $\mathcal{D}_{ls}(t)$, respectively, from left to right and top to bottom. The solid lines are quark propagators and the solid circles γ_5 insertions.

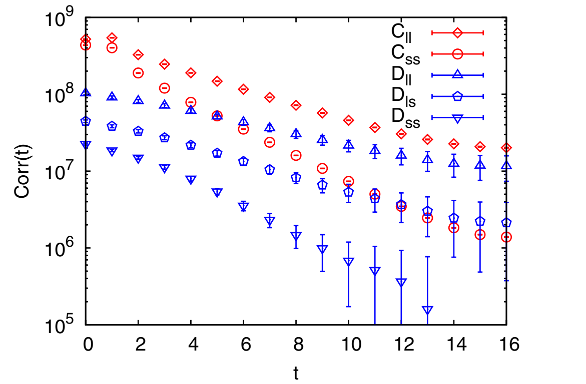

FIG. 2 (color online). Results for the five contractions which enter the $\eta - \eta'$ correlator calculated by using the $m_l = 0.01$ ensemble.

the disconnected graphs, large statistics are required. Therefore, we calculate propagators for sources on each of our 32 time slices. The large number of Dirac operator inversions (32×12) that must be performed on a single gauge configuration is accelerated by computing the Dirac eigenvectors with the smallest 35 ($m_l = 0.01$) or 25 ($m_l = 0.02, 0.03$) eigenvalues and limiting the conjugate gradient inversion to the remaining orthogonal subspace. This results in a 60% speedup for $m_l = 0.01$. We study 300 configurations separated by 10 molecular dynamics time units for $m_l = 0.01$ and 0.02 and 150 configurations separated by 20 time units for $m_l = 0.03$.

We compute four Euclidean space correlation functions between two pseudoscalar operators O_l and O_s:

$$C(t)_{\alpha\beta} = \frac{1}{32}\sum_{t'=0}^{31}\langle O_\alpha(t+t')^\dagger O_\beta(t')\rangle, \qquad \alpha, \beta \in \{l, s\}, \quad (1)$$

summed over the 32 source locations. Here $O_s = \bar{s}\gamma_5 s$ and $O_l = (\bar{u}\gamma_5 u + \bar{d}\gamma_5 d)/\sqrt{2}$, both SU(2) singlets.

The matrix $C(t)$ can be expressed in terms of the five amplitudes represented by the diagrams shown in Fig. 1:

$$\begin{pmatrix} C_{ll} & C_{ls} \\ C_{sl} & C_{ss} \end{pmatrix} = \begin{pmatrix} \mathcal{C}_{ll} - 2\mathcal{D}_{ll} & -\sqrt{2}\mathcal{D}_{ls} \\ -\sqrt{2}\mathcal{D}_{sl} & \mathcal{C}_{ss} - \mathcal{D}_{ss} \end{pmatrix}. \quad (2)$$

This equation shows that neither O_l nor O_s creates an energy eigenstate of QCD. They mix with each other through the disconnected diagram $\mathcal{D}_{sl} = \mathcal{D}_{ls}$. The usual expectation that such disconnected graphs are small does not apply here. Figure 2 shows these amplitudes versus time for the $m_l = 0.01$ ensemble. The disconnected graphs decrease more slowly than the connected graphs, changing the pattern of SU(3) flavor symmetry breaking.

Inserting a sum over states into Eq. (1) and assuming this sum is dominated by the η and η' for large t, we obtain

$$C(t) = A^T D(t) A, \quad (3)$$

where the overlap matrix A is given by

$$A = \begin{pmatrix} \langle \eta|O_l|0\rangle & \langle \eta|O_s|0\rangle \\ \langle \eta'|O_l|0\rangle & \langle \eta'|O_s|0\rangle \end{pmatrix}, \quad (4)$$

and $D(t)$ is a diagonal matrix with elements $e^{-m_\eta t}$ and $e^{-m_{\eta'} t}$. We chose A real, possible because $C(t)$ is real.

Now define a second operator basis with definite SU(3) properties: the octet $O_8 = (\bar{u}\gamma^5 u + \bar{d}\gamma^5 d - 2\bar{s}\gamma^5 s)/\sqrt{6}$ and the singlet $O_1 = (\bar{u}\gamma^5 u + \bar{d}\gamma^5 d + \bar{s}\gamma^5 s)/\sqrt{3}$. We will use the Roman indices a and b, for these operators, e.g., $\{O_a\}_{a=8,1}$, to distinguish them from the earlier basis $\{O_\alpha\}_{\alpha=l,s}$. Equations analogous to Eqs. (1), (3), and (4) will be obeyed if this second basis with $ab \in \{8, 1\}$ is used.

We can determine the two masses and the four real elements of the matrix A by fitting our data to Eq. (3) over an appropriate range of time t. To determine this range we examine the product:

$$C(t_0)^{-1}C(t) = A^{-1}D(t - t_0)A, \quad (5)$$

implying $C(t_0)^{-1}C(t)$ is similar to a diagonal matrix whose eigenvalues are exponentials of the masses of interest. We find the best results if $t - t_0$ is large, giving a clean separation of the larger, more accurate η eigenvalue and the smaller eigenvalue associated with the noisy η'. Figure 3 shows the eigenvalues obtained from Eq. (5). Here we plot the logarithm of the ratio of each eigenvalue evaluated at t and $t + 1$ with $t_0 = 2$. The choice $t_0 = 2$ and $3 \le t \le 7$ gives a recognizable plateau for m_η and $m_{\eta'}$.

$\eta - \eta'$ mixing.—It is customary to treat the physical η and η' states as mixtures of the pseudoscalar octet and singlet states which appear in the SU(3) symmetric limit and to introduce an angle θ which specifies this mixing. In the present calculation we can examine the validity of this mixing model and attempt to determine θ. Consider the SU(3) symmetric limit $m_l = m_s$ and let $|8\rangle_{\mathrm{sym}}$ and $|1\rangle_{\mathrm{sym}}$ be these lowest energy octet and singlet states with energies E_8 and E_1. We justify this mixing model by assuming that when $m_l \neq m_s$ the only important effects are a subset of those implied by first-order perturbation theory: first-order

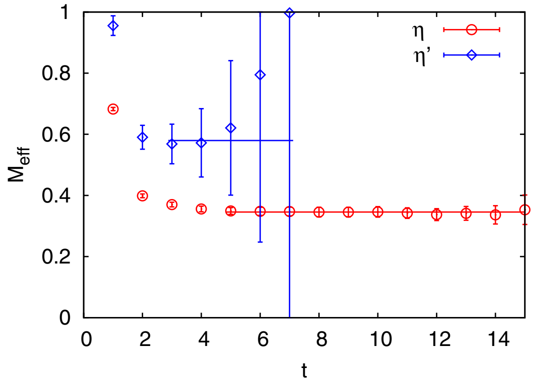

FIG. 3 (color online). Effective mass plot for the η and η' states from the $m_l = 0.01$ ensemble.

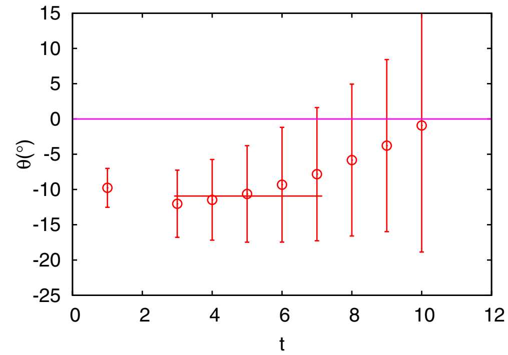

FIG. 4 (color online). The $\eta - \eta'$ mixing angle $\theta(t)$ determined from Eq. (5) for the $m_l = 0.01$ ensemble. While the errors are large, the data are consistent with a single value of about $-10°$ for $3 \le t \le 7$. [Note that $\theta(t)$ is undefined at $t_0 = 2$ and off scale at $t = 0$.]

energy shifts and first-order mixing of states but only for those cases enhanced by the relatively small energy denominator $E_1 - E_8$. To zeroth order in $m_s - m_l$ we can write ${}_{\rm sym}\langle a|O_b|0\rangle = Z_a^{1/2}\delta_{ab}$, and we assume this relation is unchanged by the first-order effects of $m_s - m_l$ on the vacuum state—again neglecting mixing not enhanced by the factor $1/(E_1 - E_8)$.

These assumptions imply that

$$\begin{pmatrix} |\eta\rangle \\ |\eta'\rangle \end{pmatrix} = \begin{pmatrix} \cos(\theta) & -\sin(\theta) \\ \sin(\theta) & \cos(\theta) \end{pmatrix} \begin{pmatrix} |8\rangle_{\rm sym} \\ |1\rangle_{\rm sym} \end{pmatrix} \tag{6}$$

and that the overlap matrix A can be written

$$A = \begin{pmatrix} Z_8^{(1/2)}\cos(\theta) & -Z_1^{(1/2)}\sin(\theta) \\ Z_8^{(1/2)}\sin(\theta) & Z_1^{(1/2)}\cos(\theta) \end{pmatrix}, \tag{7}$$

for A in the $O_8 - O_1$ basis. The columns of A are thus orthogonal and, if O_8 and O_1 are normalized by multiplication by $Z_8^{-1/2}$ and $Z_1^{-1/2}$, the resulting overlap matrix $\hat{A}$ will be orthogonal. Using the results below, we find for the dot product between the columns of $\hat{A}$ $-0.016(9)$ and $-0.012(4)$ for the $m_l = 0.01$ and 0.02 ensembles, respectively.

We can also extract an effective mixing angle $\theta(t)$ from Eq. (5). This equation determines each row of A up to an arbitrary constant. However, these two undetermined normalization factors as well as the factors $Z_8^{1/2}$ and $Z_1^{1/2}$ cancel from the product $A_{\eta 1}A_{\eta' 8}/A_{\eta 8}A_{\eta' 1}$, a combination which equals $-\tan^2(\theta)$. The resulting angle is shown in Fig. 4. The small value of θ in the O_8 and O_1 basis demonstrates the large role played by the disconnected diagrams. Had we omitted the disconnected diagrams, the matrix A would have been diagonal in the O_l and O_s basis giving $\sin(\theta) = -\sqrt{2/3}$ or $\theta = -54.7°$, very different from our $\theta = -14.1(2.8)°$.

Fitting results.—We fit our four correlation functions $C_{ab}(t)$ in two steps. First, using $3 \le t \le 7$ we determine the two masses m_η and $m_{\eta'}$ and the four elements of A. Second, we fix A to that determined in the first step and fit the $\eta\eta$ element of the transformed matrix $[(A^T)^{-1}C(t)A^{-1}]_{\eta\eta}$ over the larger range $5 \le t \le 15$ to determine more accurately m_η. For each fit we minimize χ^2 computed from the full covariance matrix, which includes the statistical correlations between each measured propagator at each of the time separations used. We treat each configuration as independent but check for autocorrelations by grouping the data into blocks of size up to 10 and find consistent errors. As a test for long autocorrelations, we compare the first and second halves of our data and find consistent results. Using random sources, Refs. [8,15] suggest these disconnected correlators show large statistical excursions. We do not see this behavior. Our standard wall sources give disconnected and connected propagators which follow similar, properly sampled distributions.

For the $m_l = 0.03$ ensemble, we reweight the correlation functions to change $m_s^{\rm sea}$ from 0.04 to 0.032 and list the results in Table I. We then linearly interpolate the resulting m_η^2 and $m_{\eta'}$ with strange valence quark masses of 0.03 and 0.04 to the point $m_s^{\rm val} = 0.032$. Table II lists the resulting

TABLE I. Meson masses for the $m_l/m_s = 0.03/0.04$ ensemble and at the reweighted value $m_s^{\rm sea} = 0.032$ for two values of the valence strange quark mass $m_s^{\rm val} = 0.03$ and 0.04. Here and below, only jackknife, statistical errors are given.

$m_s^{\rm sea}$	m_π	$m_s^{\rm val}$	m_η	$m_{\eta'}$
0.04	0.3907(9)	0.03	0.3907(9)	0.716(49)
		0.04	0.4316(16)	0.713(67)
0.032	0.3899(11)	0.03	0.3899(11)	0.688(60)
		0.04	0.4328(20)	0.694(126)

TABLE II. Masses in lattice units for the nonet of pseudoscalar mesons.

m_l(conf)	m_π	m_K	m_η	$m_{\eta'}$	θ	m_η(Gell-Mann–Okubo)
0.01(300)	0.2441(7)	0.3272(7)	0.3572(24)	0.600(45)	$-8.3(2.6)°$	0.3505(10)
0.02(300)	0.3251(6)	0.3633(6)	0.3787(11)	0.605(36)	$-5.5(1.4°)$	0.3752(9)
0.03(150)	0.3899(11)	⋯	0.3988(13)	0.689(73)	⋯	⋯

masses for the octet states π, K, and η and the singlet state η' for each ensemble. The final column shows m_η determined by the Gell-Mann–Okubo formula $3m_\eta^2 + m_\pi^2 = 4m_K^2$ using our values for m_π and m_K. The good agreement with this first-order formula is consistent with our small octet-singlet mixing.

In Fig. 5, we show a linear extrapolation of $m_{\eta'}$ and m_η^2 as a function of m_π^2 to the physical value of m_π, consistent with next-to-leading-order chiral perturbation theory. (Note that the curvature of the m_η fit is barely visible.) We find $m_\eta = 573(6)$ MeV and $m_{\eta'} = 947(142)$ MeV, where the errors are statistical. To verify our choice of m_s, we extrapolate the kaon mass and find the physically consistent value 497.4(7) MeV. Also shown is a similar linear extrapolation for θ giving $\theta = -14.1(2.8)°$, in agreement with the range $-10°$ to $-20°$ of phenomenological values [16].

We have described a $2 + 1$-flavor calculation of the masses and mixing for the η and η' mesons, finding results agreeing within their 15% error with experiment. The near orthogonality of the mixing matrix $\hat{A}$ is consistent with physical states which are simple mixtures of SU(3) octet and singlet states. Given our large statistical errors, we have not analyzed the smaller systematic errors arising from our single lattice spacing, large light quark masses, and finite volume which other calculations [11,13,17] suggest are $\approx 4\%$, 5%, and 1%, respectively. However, to this accuracy our calculation demonstrates that QCD can explain the large mass of the ninth pseudoscalar meson and its small mixing with the SU(3) octet state.

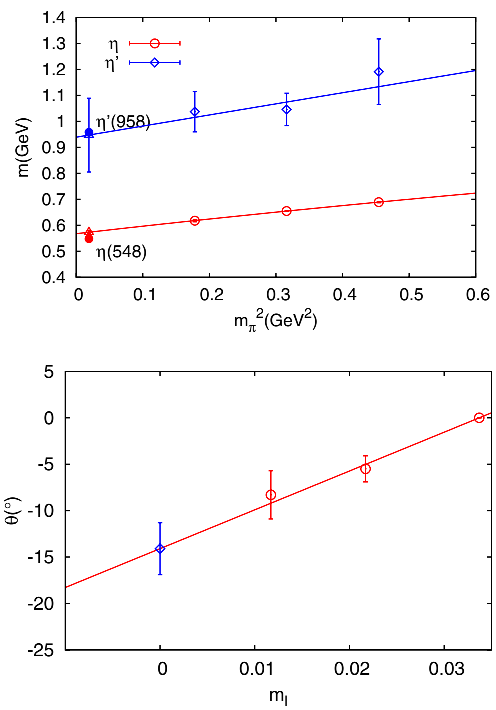

FIG. 5 (color online). Extrapolation of m_η, $m_{\eta'}$ (upper), and θ (lower) to the physical light quark mass (and a negative input mass m_l).

We thank our RBC/UKQCD collaborators for many helpful ideas and BNL, the University of Edinburgh, PPARC, and RIKEN for providing the facilities on which this work was performed. This work was supported by STFC Grant No. ST/G000557/1, EU Contract No. MRTN-CT-2006-035482 (Flavianet), U.S. DOE Grants No. DE-AC02-98CH10886 and No. DE-FG02-92ER40699, and JSPS Grant-in-Aid No. 19740134 and No. 22540301.

[1] S. Weinberg, Phys. Rev. D **11**, 3583 (1975).
[2] A. A. Belavin, A. M. Polyakov, A. S. Schwartz, and Y. S. Tyupkin, Phys. Lett. **59B**, 85 (1975).
[3] G. 't Hooft, Phys. Rev. Lett. **37**, 8 (1976).
[4] Y. Kuramashi, M. Fukugita, H. Mino, M. Okawa, and A. Ukawa, Phys. Rev. Lett. **72**, 3448 (1994).
[5] L. Venkataraman and G. Kilcup, arXiv:hep-lat/9711006.
[6] C. McNeile and C. Michael (UKQCD Collaboration), Phys. Lett. B **491**, 123 (2000); **551**, 391(E) (2003)
[7] L. Del Debbio, L. Giusti, and C. Pica, Phys. Rev. Lett. **94**, 032003 (2005).
[8] K. Jansen, C. Michael, and C. Urbach (ETM Collaboration), Eur. Phys. J. C **58**, 261 (2008).
[9] K. Hashimoto and T. Izubuchi, Prog. Theor. Phys. **119**, 599 (2008).
[10] S. Aoki *et al.* (JLQCD Collaboration), Proc. Sci., LAT2006 (2006) 204 [arXiv:hep-lat/0610021].
[11] C. Allton *et al.* (RBC-UKQCD Collaboration), Phys. Rev. D **78**, 114509 (2008).
[12] C. Allton *et al.* (RBC and UKQCD Collaborations), Phys. Rev. D **76**, 014504 (2007).
[13] R. Mawhinney (RBC and UKQCD Collaborations), Proc. Sci., LAT2009 (2009) 081 [arXiv:0910.3194].
[14] C. Jung, Proc. Sci., LAT2009 (2009) 002 [arXiv:1001.0941].
[15] E. B. Gregory, A. C. Irving, C. M. Richards, and C. McNeile, Phys. Rev. D **77**, 065019 (2008).
[16] T. Feldmann, Int. J. Mod. Phys. A **15**, 159 (2000).
[17] C. Kelly *et al.* (RBC and UKQCD Collaborations), Proc. Sci., LAT2009 (2009) 087 [arXiv:0911.1309].